

LA-5604-MS  
Informal Report

UC-34  
Reporting Date: April 1974  
Issued: June 1974

ic. 3

CIC-14 REPORT COLLECTION  
**REPRODUCTION  
COPY**

**Ablation Stability of  
Laser-Driven Implosions**

by

D. B. Henderson  
R. L. McCrory  
R. L. Morse



This report is based on a paper presented at the 7th European Conference on Plasma Production by High-Power Lasers at Garching bei München, April 22-26, 1974.



**los alamos**  
**scientific laboratory**  
of the University of California  
LOS ALAMOS, NEW MEXICO 87544

This report was prepared as an account of work sponsored by the United States Government. Neither the United States nor the United States Atomic Energy Commission, nor any of their employees, nor any of their contractors, subcontractors, or their employees, makes any warranty, express or implied, or assumes any legal liability or responsibility for the accuracy, completeness or usefulness of any information, apparatus, product or process disclosed, or represents that its use would not infringe privately owned rights.

In the interest of prompt distribution, this LAMS report was not edited by the Technical Information staff.

Printed in the United States of America. Available from  
National Technical Information Service  
U.S. Department of Commerce  
5285 Port Royal Road  
Springfield, Virginia 22151  
Price: Printed Copy \$4.00 Microfiche \$1.45

# ABLATION STABILITY OF LASER-DRIVEN IMPLOSIONS

by

D. B. Henderson, R. L. McCrory, and R. L. Morse

## ABSTRACT

We extend the perturbation analysis of laser-driven implosions showing the positive stability of the ablation surface. (The opposite conclusion has been reported by others). We present numerical results from a more complete class of problems. Our conclusions are supported by general physical arguments.

Recent interest in laser-driven implosion of spherical pellets of thermonuclear fuel to high densities has raised important questions about the symmetry and stability of such implosions. It has been observed by Henderson and Morse<sup>1</sup> that small departures from spherical symmetry of the coupled hydrodynamic and heat flow processes involved can be analyzed by a linear perturbation expansion in scalar spherical harmonics,  $Y_l^m(\hat{\Omega})$ , and that the analysis is greatly simplified by a decoupling of equations for different  $l$ 's and a degeneracy with respect to the  $m$ 's. This mathematical technique has been applied to the analysis of implosion asymmetries caused by nonuniform laser irradiation of DT pellets by Henderson and Morse.<sup>2</sup> They also stated in Ref. 2, but do not show, that similar calculations indicate positive stability of the ablation process by which absorbed energy causes the implosion. Shiau, Goldman, and Weng,<sup>3</sup> using the same mathematical technique with a similar but not identical numerical method, have reached the opposite conclusion. We present here a complete calculation of the coupled zero-order (radial) and first-order (perturbed) problem. Three different kinds of problems have been done: an initial deformation corresponding to bumpy surfaces; an initial deformation corresponding to granularity or bubbles (nonuniform density); and boundary conditions corresponding to nonuniform laser

illumination. Examples are shown of the first and last. All three yield the conclusion that the ablation surface is stable, as mentioned in Ref. 2. Physical arguments are presented which support this conclusion.

The zero-order spherical implosion case chosen here as our example was taken from a study of implosions of 500  $\mu\text{m}$  radius frozen DT spheres isotropically irradiated by Gaussian laser pulses with a wavelength of 1.06  $\mu\text{m}$ . The zero-order computations were done by a single temperature Lagrangian hydrodynamics code with electron thermal conduction. Figure 1a is a contour plot of the maximum central densities achieved as a function of the total pulse energy,  $E$ , and the full width of the pulse at half maximum,  $\tau$ . Figure 1b is a plot of the corresponding center temperatures at the times of maximum density. The circled points indicate the case chosen,  $E = 50$  kJ,  $t = 5.5 \times 10^{-10}$  sec. This case, which is on the long pulse side of that value of  $\tau$  which gives the maximum density for the chosen value of  $E$ , produces a shock clearly separated from the ablation surface and a shocked region in between that is much cooler than the blow-off plasma during most of the implosion. In Figs. 2a and b the zero-order density and temperature,  $\rho_0$  and  $T_0$ , are plotted at three different times ( $t = -0.21 \times 10^{-9}$ ,  $+ 0.24 \times 10^{-9}$  and  $+ 0.53 \times 10^{-9}$  s with respect to the



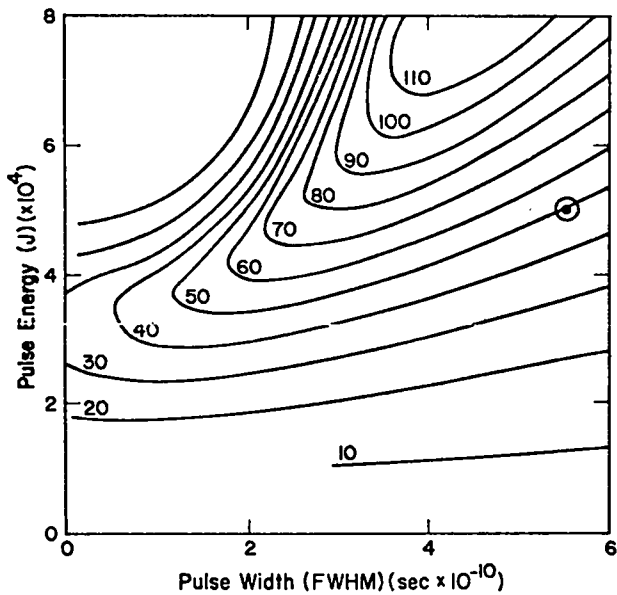


Fig. 1a. Contours of maximum center density in  $\text{g/cm}^3$  at time of maximum density as a function of pulse energy  $E$ , and full width  $\tau$  at half maximum. Circled points indicate the example case.

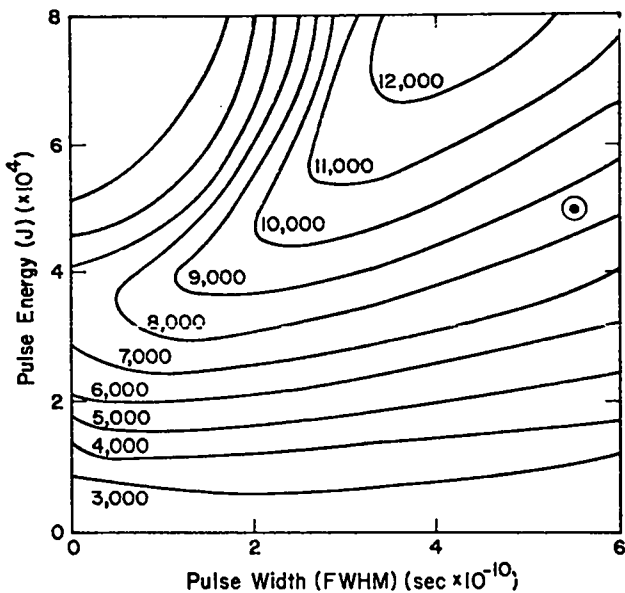


Fig. 1b. Contours of temperature in eV at time of maximum density as a function of pulse energy  $E$ , and full width  $\tau$  at half maximum. Circled points indicate the example case.

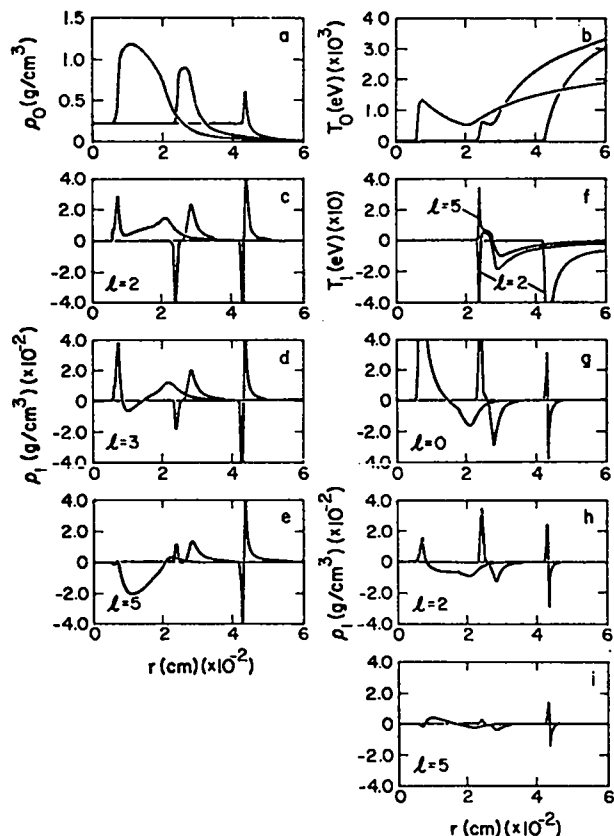


Fig. 2. Zero- and first-order quantities as a function of  $r$  at times  $t = 0.21, + 0.24, + 0.53 \times 10^{-9}$  with respect to the peak of the Gaussian pulse.

peak time of the Gaussian pulse, on the same axes. Going out from  $r = 0$ , the shock is where  $\rho_0$  and  $T_0$  rise sharply, the ablation front is where  $\rho_0$  subsequently falls sharply just outside its maximum and  $T_0$  begins to rise again). This class of implosion is quite similar to those produced by highly optimized pulses up to a time just before peak compression (See Refs. 2 and 3 for further references). Values of  $\tau$  near the maximum density value or on the short side give implosions in which the ablation and shock surfaces are not so clearly separated, the region just behind the shock is not very much cooler than the blow-off plasma, and the resulting higher thermal conductivity in this region further increases the stability of the flow. It is not asserted that this case

is the least stable possible case but rather that this case is representative of those relevant to laser fusion. We do not know of a relevant class of homogeneous pellet cases which we expect would be significantly less stable.

Angle dependent first-order perturbations of all zero-order dependent variables are represented by time and radius dependent coefficients of spherical harmonics of various  $\ell$ -values, and are calculated by integration along the unperturbed characteristics of the zero-order Lagrangian flow, according to the method described in Ref. 2. Ablation stability is isolated from effects of illumination asymmetry by assuming symmetric irradiation and an initial perturbation of the pellet of the incompressible form:

$$\xi_r = \xi_0 (r/a)^{\ell-1}$$

$$(\nabla \cdot \xi)_\Omega = -(\ell + 1) (\xi_0/a) (r/a)^{\ell-2},$$

which gives the pellet a bumpy surface. The unperturbed radius of the pellet is  $a$ , which is  $500 \mu\text{m}$  for the case shown here. The scale of all first-order quantities is set by taking  $\xi_0 = 1 \mu\text{m}$ , and thus giving the bumpy surface this amplitude. We prefer this form of regular initial perturbation over the random noise approach of Shiau et al.<sup>3</sup> for estimating the effect of initial pellet irregularities and any instability on implosion symmetry. Figures 2c, d, and e show the perturbed density coefficients,  $\rho_1$ , for  $\ell = 2, 3$ , and  $5$ , respectively, at the same three times at which  $\rho_0$  and  $T_0$  are plotted. At  $t = -.21 \times 10^9$  sec for all  $\ell$ 's, the inside negative spike of  $\rho_1$ , which is well resolved by our grid, comes mostly from the convective contribution given by the product of the large  $\partial\rho_0/\partial r$  at the shock and of  $-\xi_r$  there. The negative sign of the spike reflects the fact that at the angular phase  $\cos\theta = 1$ , where first-order quantities are defined and, in general, wherever  $Y_\ell^m(\bar{\Omega}) > 1$ , the perturbed surface is initially raised, i.e., displaced outward, and the inward progress of the shock is retarded at early times relative to the zero-order flow by having to pass through additional material. The outward displacement of the critical surface, in the vicinity of where the light is absorbed also contributes to shock retardation at

this angular phase. Artificial viscosity distributes the shock jump, which is in principle discontinuous, over enough zones to permit accurate calculation of  $\rho_1$  and other first-order quantities. The area under this spike is a measure of the perturbed radial shock displacement. The rest of  $\rho_1$  behind the shock can be taken at face value. The positive feature of  $\rho_1$  at  $t = -0.21 \times 10^{-9}$  for all  $\ell$ 's is also primarily convective, reflecting the initial outward displacement and the negative  $\partial\rho_0/\partial r$  of the ablation front.

Subsequently, the following sequence of events occurs for all  $\ell > 1$ . Angular thermal conduction increases the total heat flow into the regions of  $\bar{\Omega}$  in which the surface of the pellet is initially raised, causing material to be ablated from these regions with greater energy, i.e., with greater specific impulse. The greater ablation pressure in the initial raised regions of  $\bar{\Omega}$  causes the shock to be stronger there and hence to produce a higher shocked pressure behind and to move inward faster. The shock in the initially depressed regions of  $\bar{\Omega}$  is correspondingly weaker and slower than the zero-order shock. The shock in the raised regions, which starts out retarded, in fact catches up with and moves ahead of the zero-order shock. This is first seen for  $\ell = 5$  in Fig. 2e at  $t = .24 \times 10^{-9}$  from the sign reversal of the spike in  $\rho_1$  at the shock front from negative at the earlier time to positive. The same transition is seen to occur between  $t = 0.24 \times 10^{-9}$  and  $t = 0.53 \times 10^{-9}$  for  $\ell = 2$  and  $3$ . This motion of the shock front from one side of its zero-order position to the other might be expected to exhibit overstability, but this has not been observed. Thus, the observed behavior is positively stable. The reversal of shock retardation occurs sooner at higher  $\ell$ -numbers because the angular wavelength is shorter and the angular thermal conduction is larger, as discussed in detail in Ref. 2.

The angular variation of perturbed pressure behind the shock front also causes a perturbed angular fluid flow which decreases the density in the initially raised regions of  $\bar{\Omega}$ . This density decrease is seen in a fully developed state at  $t = 0.53 \times 10^{-9}$  for  $\ell = 5$  and it is beginning to occur for  $\ell = 3$ . The above behavior corresponds to a tendency for the implosion to converge to

separate points located on those radii on which there occurred initial minima of the pellet surface radius, i.e., minima of  $Y_{\ell}^m(\bar{\Omega})$ , as opposed to converging uniformly to the spherical center. This tendency to form local density maxima in the imploding shell of compressed material can be seen from the fact that Fig. 2e at  $t = 0.53 \times 10^{-9}$  exhibits a negative maximum of  $\rho_1$  at the same radius as the maximum of  $\rho_0$  (Fig. 2a). (If, on the other hand, the maximum of  $\rho_1$  occurred in either on the regions of large  $\pm \partial \rho_0 / \partial r$  and if the zeros of  $\rho_1$  and  $\partial \rho_0 / \partial r$  coincided, it would instead indicate only a waviness of the surface of maximum density with no isolated points of maximum density of this surface). Figure 2f helps in visualizing the ablation stabilization process described above. On the scales are plotted  $T_1$  for  $\ell = 2$  at  $t = 0.21 \times 10^{-9}$  and  $T_1$  for  $\ell = 2$  and  $5$  at  $t = 0.24 \times 10^{-9}$ . The major contribution to  $T_1$  ( $\ell = 2$ ,  $t = -0.21 \times 10^{-9}$ ) is from retardation of the nonlinear thermal wave form of  $T_0$  (Fig. 2b) at this time. ( $T_1$  for  $\ell = 3$  and  $5$  at this time are almost identical to  $\ell = 2$ ). However, between  $t = -.21 \times 10^{-9}$  the angular conduction damping of  $T_1$  in the vicinity of the ablation front is significantly greater for higher  $\ell$ 's. Thus, at  $t = .24 \times 10^{-9}$  in this vicinity the negative magnitude of  $T_1$  ( $\ell = 5$ ) is noticeably smaller than that of  $T_1$  ( $\ell = 2$ ). However, in the shocked layer, where  $\ell = 2$  and  $5$  are positive and almost flat, the magnitude of  $T_1$  ( $\ell = 5$ ) is greater, indicating stronger shocking as described above. The spike-like features nearest the origin are indicators of the perturbed shock displacement, just as are the corresponding  $\rho_1$  features, and have opposite signs at this time because the  $\ell = 5$  shock has crossed over and  $\ell = 2$  has not.  $T_1$  ( $\ell = 3$ ,  $t = 0.24 \times 10^{-9}$ ) lies everywhere between  $\ell = 2$  and  $\ell = 5$ . Inspection of  $(\vec{v} \cdot \vec{E})_{\bar{\Omega}}$  shows that the additional curvature of the surface introduced by the surface perturbation also contributes to strengthening the shock and speeding the implosion in the initially raised regions of  $\bar{\Omega}$  by making the implosion at early times converge more rapidly than in zero-order, as if converging to points out from the origin on radii passing through initial maxima of  $Y_{\ell}^m(\bar{\Omega})$ . This purely hydrodynamic effect may make an important contribution to increasing the symmetry of imploding shells of fuel.

Regular initial perturbation of internal density gives results very similar to those obtained from regular surface perturbations.

In order to learn the relative contributions of initial surface perturbations and of perturbations of illumination uniformity to implosion asymmetry, we have calculated the perturbed response of our same zero-order case to angular radiation variations scaled here to a relative modulation of  $10^{-2}$ . Figures 2g, h, and i show the results for  $\ell = 0, 2$ , and  $5$  at the same times as above. Comparison of such  $\ell = 0$  calculations with appropriately defined differences between two zero-order runs with only slightly different input power provides an extremely valuable verification of the numerical method. The  $\ell = 2$  and  $5$  results show the smoothing effect of higher  $\ell$ 's pointed out in Ref. 2 although without the distinction made there between early and late time irradiation asymmetry. Comparison shows that for  $\ell = 2$  the magnitude of the late time effect of an initial  $1 \mu\text{m}$  surface radius perturbation amplitude on this  $500 \mu\text{m}$  radius pellet (0.2%) is approximately the same as that caused by a 1% variation of illumination intensity.

Similar calculations of the effects of these kinds of perturbation (incompressible bumpiness, perturbed density, and asymmetric illumination) have been done with  $50 \mu\text{m}$  pellets with qualitatively very similar results.

#### ACKNOWLEDGMENTS

The authors wish to acknowledge extensive discussion of the arguments presented above with the other members of the Los Alamos laser project experimental and theoretical groups and, in particular, with the project director, Keith Boyer. We also appreciated numerous discussions with the participants at the 7th European Conference on Plasma Production by High Power Laser and, in particular, with Stewart Ramsden and Keith Brueckner.

#### REFERENCES

1. D.B. Henderson and R.L. Morse, Bull. Amer. Soc. Ser. II 18 684 (April 1973). This material was previously presented to the laser fusion community at the L.F.C.C. meeting in Livermore, Jan. 1973.
2. R.L. Morse, Bull. Amer. Phys. Soc., Ser. II, 18, 1359 (Nov. 1973) - invited paper. This paper is published as D.B. Henderson and R.L. Morse, Phys. Rev. Lett. 32, 355 (1973).
3. J. N. Shiau and E.B. Goldman, Bull. Amer. Phys. Soc., Ser. II, 18 1358 (NOV. 1973). This paper is published as J.N. Shiau, E.B. Goldman, and I.C. Weng, Phys. Rev. Lett. 32, 352 (1973).